Mechanistic Modelling of Targeted Pulmonary Delivery of Dactinomycin Iron Oxide Loaded Nanoparticles for Lung Cancer Therapy

Shahd F. Al-Tarawneh [a], Eman Zmaily Dahmash [a*], Hamad Alyami [b], Suha M. Abu-Doleh [c], Samer Al-Ali [d], Affiong Iyire [e], and Rasha Abuthawabeh [c]

[a] *Department of Applied Pharmaceutical Sciences and Clinical Pharmacy, Faculty of Pharmacy, Isra University, Amman, Jordan.*
[b] *Department of Pharmaceutical Sciences, School of Pharmacy, Najran University, Najran, Saudi Arabia*
[c] *Department of Basic Pharmaceutical Sciences, Faculty of Pharmacy, Isra University, Amman, Jordan.*
[d] Faculty of Science, Isra University, Amman, Jordan
[e] Aston Pharmacy School, College of Health & Life Sciences, Aston University, Birmingham, B4 7ET, UK.

*Corresponding author:
Dr. Eman Zmaily Dahmash
Mailing address: Faculty of Pharmacy, Isra University, Amman Jordan P.O. Box 33 Isra University Office 11622.
Orchid number: https://orcid.org/**0000-0002-9815-3720**
Mobile phone: +962797439871.
Email: eman.zmaily@iu.edu.jo

Mechanistic Modelling of Targeted Pulmonary Delivery of Dactinomycin Iron Oxide Loaded Nanoparticles for Lung Cancer Therapy

Abstract

With the increase in respiratory conditions including lung cancer post covid-19 pandemic, drug-loaded nanoparticulate dry powder inhalers (DPIs) can facilitate targeted lung delivery as a patient-friendly, non-invasive method. The aim of this work was to synthesise and optimise iron oxide nanoparticles (IONPs) containing dactinomycin as a model drug, using Quality by Design (QbD) principles. Chitosan and sodium alginate were investigated as polymeric coatings. The mass median aerodynamic diameter (MMAD), fine particle fraction (FPF), burst-effect (BE), entrapment-efficiency (EE) and the emitted-dose (ED) were investigated in initial screening studies and outcomes used to set up a Design of Experiments (DoE). Results revealed that chitosan IONPs were superior to that of sodium alginate in delivering DPI with optimal properties [ED (89.9%), FPF (59.7%), MMAD (1.59 μm) and BE (12.7%)]. Design space for targeted IONPs included formulations containing 2.1-2.5% dactinomycin and 0.5–0.9% chitosan. Differential scanning calorimetry and X-ray diffraction and SEM-EDS analysis revealed effective formation of IONPs, and TEM images revealed the production of spherical IONPs with particle size of 4.4 ± 0.77 nm. This work overcame the light sensitivity of dactinomycin to potentially target the high molecular weight drugs to the lungs, with controlled delivery based on a reduced burst effect.

Keywords: Dactinomycin; nanoparticles; iron oxide; chitosan; sodium alginate; pulmonary drug delivery.

Introduction

The world health burden of pulmonary diseases has increased since the covid-19 pandemic with over 1 billion people suffering from acute and chronic respiratory conditions, including lung cancer (Zimmermann et al. 2022). This necessitates the continuous development of novel drug delivery and targeting systems that take advantage of the large surface area, high vascularisation and thin blood-alveolar barrier of the pulmonary route for local and systemic delivery of therapeutic agents – requiring lower doses with minimised side effects (Haschek et al. 2010; Liang et al. 2015; Hill et al. 2019). In recent times, nanoparticles have been employed for targeted drug delivery of anticancer agents to reduce drug loss during transit and the associated side effects of chemotherapy (McMillan et al. 2011; Jana and Jana 2016; Singh et al. 2017). Super paramagnetic iron oxide nanoparticles (SPION) consist of a core of magnetite (Fe_3O_4) or maghemite (Fe_2O_3); coated with polymers, monomers, or polysaccharides; with functional groups attached to the surface coating to accomplish targeted delivery of particles for imaging/drug delivery for specific cells and tissue sites. Thus, SPION applied in magnetic resonance imaging (MRI) to investigate the differences between normal and abnormal/cancerous cells have been successfully developed (McMillan et al. 2011) and SPION, approximately 60-150 nm in diameter are currently the only clinically approved metal oxide nanoparticles available and have been researched for the delivery of antituberculosis and anti-cancer agents (Wang et al. 2016; Acharya et al. 2017; Kaur et al. 2017; Muthuraman and Kaur 2017; Gokduman et al. 2018).

Challenges with magnetic iron oxide nanoparticles relate to their inability to cross the blood-brain barrier (BBB) and the vascular endothelium (hence their application in pulmonary delivery); tendency to aggregate, unpredictable pharmacokinetics and rapid clearance by the mononuclear phagocytic system (also known as the reticuloendothelial system); which is dependent on their

surface properties e.g. particle size and morphology (Kammari et al. 2017). *In vivo* results revealed that after entering body cells, IONPs can accumulate in small organelles like endosomes/lysosomes, where they can augment cellular iron pools and release into the cytoplasm after decomposition. Researchers have shown that the toxicity of IONPs is mainly associated with their physicochemical properties such as size, shape, dose, time of exposure, surface chemistry, coating layers and functional groups (Han et al. 2007; Hanini et al. 2011; Wang et al. 2017). Therefore, these parameters must be closely monitored and controlled to reduce the toxicity of this very useful delivery system.

Active pharmaceutical ingredients (APIs) such as dactinomycin (**see Figure 1**), the antibiotic/antitumour drug, formulated as nanoparticles, can be delivered to the alveoli of the lungs via different approaches such as: an environment friendly propellant in pressurized metered dose inhalers (pMDIs), non-aqueous inhalers also known as dry powder inhalers (DPIs), and jet or ultrasonic nebulizers. To deliver micronised and aerosolised drug particles in an effective manner from these devices, drug particles should be in the fine particle size range (1-5μm), possess innate electrostatic charges and ensure that sufficient API concentrations for the desired therapeutic effect can be deposited on the lungs in a reproducible manner (Kulkarni 2009; Zimmermann et al. 2022). To model lung deposition of APIs *in vitro*, the Next Generation Impactor (NGI) (**see Figure 2**) consisting of multiple size cut-off chambers that depict how far particles would travel within the lungs, is used.

[Figure 1 near here]

[Figure 2 near here]

A quality by design (QbD) approach incorporating design of experiments (DoE) closely monitors manufacturing processes to ensure that quality is built/designed into formulations and not just tested at the end of the manufacturing process (Dahmash et al. 2018). Identifying the critical process parameters that when carefully controlled and monitored would influence the critical quality attributes of the IONPs, ensures the right quality target profile (QTP) of the formulations is achieved. Therefore, the aim of this work was to develop dry powder inhalers containing IONPs loaded with a model drug – dactinomycin – for targeted drug delivery to the lungs for treatment of solid tumours. The project employed QbD principles for synthesis of IONPs, subsequent optimisation of the loading and production of effective DPIs with a QTP that delivers high fine particle fraction (FPF), high emitted dose and ensures targeting to designated areas within the lungs, using the NGI. The design space providing the range of API concentration, polymer type and concentration to yield IONPs with optimal properties, was elucidated.

Materials and Method

Materials

Dactinomycin was purchased from Sigma Aldrich (UK). Ethanol and acetone were obtained from Alpha Chemika (India). Glycerine, acetic acid, and water for HPLC were purchased from Labchem (NJ, USA). Sodium acetate was obtained from CDH fine chemicals Ltd. (New Delhi, India) while acetonitrile was obtained from Honeywell Specialty Chemicals (Seelze, Germany) and sodium hydroxide from AZ chemicals (Karachi-Pakistan). Ferrous chloride was purchased from GPR (England) and ferric chloride obtained from Guangdong Guanghua (China). Chitosan (low molecular weight 10-120 kDa, 90% deacetylation) was purchased from Sigma Aldrich (UK) and sodium alginate (Na alginate) (low viscosity 10-80 kDa) was purchased from Xilong Chemicals (China).

High Performance Liquid Chromatograph (HPLC) Assay Method for Dactinomycin

HPLC method was employed for the quantitative analysis of dactinomycin in solution. A Dionex Softron HPLC System from Thermo fisher Scientific Inc., with gradient pump, UV detector set at 254 nm was used, employing a reversed phase 5 µm, Fortis-C18 analytical column (Fortis technologies Ltd C 18. 300 x 3.9 mm). The analytical method was based on USP official monograph method (USP-35 2011) with modification where the mobile phase consisted of 46: 25: 25 of acetonitrile, 0.07 M acetic acid and 0.04 M sodium acetate. Pump flow rate was set at 1 mL/min, with sample injection volume of 50 µL. The HPLC method was validated according to ICH guidelines in terms of specificity, accuracy, precision, linearity, limits of detection and limit of quantification (ICH 2005).

Preparation of Iron Oxide Nanoparticles (IONP)

Preparation of IONP was carried out using the bottom-up method where particles are built based on chemical reaction of two main forms of iron: ferrous chloride ($FeCl_2$) and ferric chloride ($FeCl_3$) (Hussein-Al-Ali et al. 2014). 2.43 g of $FeCl_3$ and 0.89 g $FeCl_2$ were accurately weighed using BEL Engineering balance (Italy). The powders were added to 30 ml water then 1 mL of 2 M HCl was added, after complete dissolution, the solution was made up to 100 mL with water forming solution 1. In a 250 mL beaker, 100 mL of 2 M NaOH (solution 2) was added. Solution 1 was then added dropwise to solution 2. The pH value was monitored while adding solution 1 and was maintained above 10 using NaOH as needed. The colour changed from brown to black forming a dispersion described as solution 3. The reaction process between the two iron chloride salts is summarized in equation 1.

$$FeCl_2 + 2\,FeCl_3 + 8\,NaOH \rightarrow Fe_3O_4 + 8\,NaCl + 4\,H_2O \quad (1)$$

The final dispersion (solution 3) was placed in a bath sonicator for 2 hours and then centrifuged for 20 minutes at 11,000 rpm. The supernatant was removed by decantation and the precipitate was collected. The washing process using 100 mL of water was repeated four times with centrifuging for 20 minutes at 11,000 rpm. The supernatant was removed by decantation and the precipitate was collected and dried in vacuum oven at 40 ℃ for 24 hours then stored in a dry container before starting the coating process with the polymer (chitosan or Na alginate).

Coating the Iron Nanoparticles with the Polymer

The accurately weighed polymer materials (chitosan or Na alginate) at three different concentrations (0.5%, 1%, 2%) were dissolved in 100 mL of water. Acetic acid was added to chitosan solutions in an increasing amount (0.5 mL, 1 mL, and 2 mL) for the 0.5%, 1% and 2% concentrations, respectively. 1 g of the prepared IONP was added to each polymer solution (chitosan or Na alginate containing solution) and placed on magnetic stirrer for 24 hours then centrifuged for 45 minutes with speed set at 7,000 rpm. The supernatant was removed by decantation and the particles were washed and re-centrifuged two times using water then left in the oven at 40℃ for 24 hours until dried.

Development of Dactinomycin, Iron Oxide Nanoparticles and Polymer Combination

To prepare dactinomycin nanoparticles, 100 mg of the polymer coated IONP was dispersed in 20 mL of ethanol. An appropriate amount of dactinomycin was dissolved in 10 mL ethanol to form 2%, 3.5% or 5% w/v solutions. In a drop wise manner, dactinomycin solution was added to polymer coated IONP, placed on a magnetic stirrer for 24 hours, then left to evaporate at room temperature. The dried particles were milled using a mortar and pestle, passed through a sieve with aperture size of 32 μm, then 10 mg of the final product was manually filled into hard shell gelatine

157 capsules, size 3 (Pharmacare, Jordan) to be analysed by the New Generation Impactor (NGI) via
158 the Aerolizer® as the inhalation device.

159 ***Content Uniformity***

160 A Dionex Softron HPLC System from Thermo fisher Scientific Inc was used to measure
161 dactinomycin content uniformity by calculating the AUC of each sample then applying it to the
162 calibration curve equation. The content of one capsule (10 mg) of the drug-nanoparticles was
163 added to 5 mL mobile phase, shaken gently to dissolve, and filtered using 0.2 µm syringe
164 membrane filter; then 50 µL of this sample was injected into the HPLC device and elution
165 measured at 254 nm.

166 ***Entrapment Efficiency (EE)***

167 Entrapment efficiency (EE) was calculated using the indirect quantification method of
168 dactinomycin in the collective supernatant obtained from the washing of the final nanoparticles.
169 The amount of free dactinomycin was analysed using the HPLC method. The %EE was calculated
170 using the following equation:

185 $$\%EE = \frac{D_t - D_f}{D_t} X\ 100 \qquad (2)$$

186 Where D_f is the free dactinomycin in the supernatant and D_t is the total amount of dactinomycin
187 used to prepare the nanoparticles.

188 ***Aerodynamic Particle Size Analysis using Next Generation Impactor (NGI)***

189 The *in vitro* deposition and aerodynamic particle size distribution analysis was accomplished
190 using the NGI (Copley Scientific Limited Model 170, UK). A flow rate over 4 seconds to provide
191 4 litres was obtained by setting the flow rate at 60 L/min. Aerosolisation performance of

dactinomycin-IONP was determined using a Aerolizer® device with a size 3 capsule manually filled with 10 mg (±10%) of blended formulation. Six capsules were used, per test, to ensure accurate quantification of ingredients. For the quantification of dactinomycin and the calculation of both fine particle fraction (FPF) and emitted dose (ED), samples were collected at each stage of the NGI by dissolving content of each tray in 15 mL of the mobile phase, the samples were then transferred to volumetric flasks and filtered using 0.45 µm membrane filters. Then, 50 µL of the sample were injected to the HPLC to be analysed, in order to ensure stability, samples were stored at -20 ℃ and covered by aluminium foil to protect from light.

The first key aerodynamic parameter was the emitted dose (ED), which represents the total amount of API that is discharged from the capsule and deposited onto the respiratory system. The ED was calculated from the cumulative amount of dactinomycin collected from the induction tube, pre-separator, and trays 1-7 plus the final Micro Orifice Collector (MOC) of the NGI based on equation 3.

$$\text{ED}\ (\%) = \frac{\text{Cummulative content}}{\text{TM}}\, x\ 100 \qquad (3)$$

Where TM is the total amount of dactinomycin in each sample that was calculated based on entrapped percentage. The second parameter was fine particle fraction (FPF) of the emitted dose, which is calculated from the total amount of dactinomycin that was collected from trays 2-7 divided by the emitted dose in the NGI representing particles with a size range of 1-5 µm (hence the fraction that reaches the lower part of the respiratory system). Thirdly, FPF of the theoretical dose was estimated, which was calculated from the FPF divided by total amount of the drug in each sample that was calculated based on entrapped percentage.

Mass Median Aerodynamic Diameter (MMAD) Calculation

The MMAD was calculated based on the USP method <601> (USP-31 2008), the flow rate equal to 60 L/min is the base of the calculations of the cut off diameter of each stage of the NGI. The quantity of dactinomycin collected from each stage (1 to 7 and MOC) was used to calculate the cumulative mass; then MMAD and geometric standard deviation (GSD) were calculated. All results were carried out in triplicates and reported as mean ±SD.

In-vitro Drug Burst Effect Studies

A total of 10 mg of each formulation were used to detect the release performance by adding it to 2 mL of phosphate buffer saline (PBS) pH 6.8, using (Microplate spectrophotometer Thermo Fisher, Finland), wavelength was set at 254 nm. The spectrophotometer was set to record one reading every 10 minutes for 24 hours. The cumulative amount of drug released to the solution was measured at pre-set time intervals at the corresponding λ-max. The method was calibrated using PBS and a calibration curve was constructed over a range of 6.25 -125 µg/mL. Burst effect was calculated based on the percentage released at 10 minutes.

Quality by Design (QbD) Analysis

Based on the initial screening studies, literature review and compendial requirements for DPI formulations, the critical quality attributes (CQA/responses) were selected for optimisation using the critical process parameters (CPP/factors). The CPPs were determined as fundamental elements to be included further in a design of experiments (DoE) investigation. Thus, CQAs were FPF, emitted dose (ED), entrapment efficiency (EE), MMAD, burst effect (% released after 10 minutes) and FPF-Theo. While API concentration (API-Con), polymer type (chitosan and Na alginate) and

polymer concentration (Pol-Conc) were found to be the factors or critical input parameters that have a vital role in production of nanoparticles with favourable quality attributes.

MODDE GO software version 12.1 (Umetrics Inc., Sweden) was employed using the statistically designed DoE study. D-Optimal design with quadratic model was selected, which was further fitted using partial least squares (PLS) method. Thereafter, the response surface model (RSM) was employed to investigate and optimise the non-linear multidimensional relationship between factors and CQA. Subsequently, 16 runs were produced by the software, that included triplicate runs to evaluate the repeatability and error estimation, to fit the quadratic model. The experiments were carried out according to the proposed run order which was given by the software to ensure randomness of the process. **Table 1** specifies the factors/ CPP and the responses/ CQA used in the DoE.

[Table 1 near here]

The design type was regular as none of the factors underwent transformation. However, various proportions of polymer concentration and API concentrations were encoded in design as -1, 0 or 1 that stand for the lowest value, intermediate value, and highest value, respectively. **Table 2** highlights the D-optimal design worksheet with the proportions of CPP, the total number of runs and the run order.

[Table 2 near here]

To consider a model as acceptable with regards to validity and reproducibility, it should be verified. Model verification was accomplished in a step wise pattern. Model terms were revised and the impact of these terms on the model was determined employing multiple verification plots. After that, insignificant terms in the model which could negatively affect the model prediction

power were eliminated. Subsequently, the verified model was employed in further analysis of the study parameters which aimed to predict the optimal design space. ANOVA was employed, which in turn presented the results as two criteria: the variance of the regression method which is expressed by the regression coefficient significance p value that should be less than 0.05; and the variance related to residuals and replicate errors which denoted by p value of the model error (lack to fit) – its value should be higher than 0.05 to assess its non-significance. Then, according to values of regression coefficient all insignificance terms were determined and eliminated to reveal the regression equations for all CQAs.

Transmission Electron Microscopy (TEM)

Morphological composition and surface features of the nanoaggregates were assessed using TEM (JEOL-JEM- 2100F, Japan) technique and high-resolution TEM (HR-TEM) attached with selected area electron diffraction. Few milligrams of the nanoaggregates (optimised formulation) were suspended in water and TEM analyses were acquired by adding approximately 10 μL of the dispersion onto a copper grid and drying for 10 hours at room temperature. The experiments were run at an accelerating voltage of 200 kV without any further modification or coating of the sample.

Scanning Electron Microscopy (SEM)

Few milligrams of the powder were sprinkled on double-adhesive carbon tape mounted on an aluminium tub. Images were captured using a JSM-IT300 (JEOL, Japan) scanning electron microscope. Samples were analysed at low vacuum without any further coating. Energy dispersive spectra (EDS) analysis was carried out for the detection of elemental composition of samples using INCA- EDS.

Differential Scanning Calorimetry (DSC)

DSC analysis was utilised to determine the compatibility of dactinomycin with the IONP-chitosan. 2 mg of either pure chitosan, IONP-chitosan or dactinomycin -chitosan-IONP was used for the test. For DSC, samples were loaded unto the aluminium pan of a DSC Q200-TA instrument. Analysis was carried out under nitrogen and thermal behaviour recorded over a temperature range of 25 – 250 °C at a heating rate of 5°C per minute.

X-Ray Powder Diffraction

X-ray diffraction analysis (XRD) of dactinomycin, IONP-chitosan coated particles and the dactinomycin-chitosan-IONP was carried out using a MiniFlex 600 benchtop diffractometer (RigaKu, Tokyo, Japan). The XRD experiments were performed over the 2θ range from 5 to 99°, with Cu Kα radiation (1.5148227 Å) at a voltage of 40 kV and a current of 15 mA. OriginPro® software was employed to analyse the scans (OriginLab Corporation, USA).

Statistical Analysis

As needed, data was generated in replicates and analysed statistically by One-Way or Two-way ANOVA from Minitab v. 18 statistical pack. Level of significance was quoted as $p<0.05$, with a confidence interval of 95%. For NGI experiments, 6 capsules were used for each formulation.

Results and Discussion

HPLC Method for Quantification of Dactinomycin

The HPLC method for dactinomycin was validated according to ICH guidelines for analytical method validation (ICH 2005; Rozet et al. 2015). Dactinomycin peak was well resolved with retention time of 23.433 ± 0.0035 minutes. There was no interference from the solvent front which

eluted at 2.063 ± 0.020 minutes. Furthermore, none of the excipients interfered with the peak of the API. To reduce API instability due to photosensitivity, all solutions were prepared immediately before analysis, the work was performed in a dark cold room, and all solutions were covered with aluminium foil to protect from light. A Beer-Lambert calibration curve was established by plotting AUC against dactinomycin concentrations that ranged from 31.25 - 1000 µg\mL. The regression equation was $\mathbf{Y = 1.1912X + 14.956}$ ($\mathbf{R^2: 0.9999}$). The limit of detection (LOD) and limit of quantification (LOQ) of dactinomycin were then determined by using standard deviation of the response and slope as stated in ICH guidelines. The calculated LOD was 17.24 µg/mL and LOQ was 52.24 µg/mL. To investigate the precision of the procedure, ten samples of 500 µg/mL dactinomycin solution were prepared and measured, and average was 101.99 ± 1.33 (RSD= 1.30%). The results showed the process is precise as the RSD was below 2%. Inter- and Intra-day reproducibility and accuracy were assessed based on the recovery method, using 7 concentrations and results as can be seen in **Table 3**; confirming good reproducibility and accuracy of the developed method.

[Table 2 near here]

Initial Screening Studies

Initial screening studies were carried out to develop dactinomycin containing iron oxide nanoparticles to be used as nanoaggregates for potential delivery as a dry powder inhaler (DPI) to the lungs. These nanoaggregates disintegrate into individual components upon deposition. Initial investigations targeted the successful development of IONP using chitosan as a polymer. The studies focused on employing iron oxide-chitosan nanoparticles to load dactinomycin and enable the potential delivery of such particles to the lower parts of the lungs using the Aerolizer® as an inhalation device.

Dactinomycin was selected as a model API owing to its pharmacological effect for the treatment of local solid tumours. Also, being a large molecule with molecular weight of 1,255.4 g/mol (Gwaltney-Brant 2010), presented an opportunity to assess a challenging molecule in nanoparticle development. Chitosan and Na alginate were chosen as model polymers as they are biocompatible, widely used in nanoparticle development, have mucoadhesive properties, aid extended release from formulations and have several reported potential applications in drug delivery to the pulmonary system (Jana and Jana 2016; Maiti and Kumari 2016).

The key target outcomes from screening studies were to produce nanoaggregates that meet the compendial requirements in terms of content uniformity and demonstrate good aerodynamic performance; to produce a successful DPI. These target outcomes included: high level of emitted dose preferably exceeding 60%; high FPF of the emitted dose, above 20%; high FPF of the theoretical dose; and a low burst effect which was measured from the low release of dactinomycin within the first 10 minutes (indicating that the drug is retained within the nanoparticles and hence will produce minimal irritation to the upper parts of the respiratory system upon inhalation) (Bhattacharjee 2020). Another key critical attribute was focused on assessing the MMAD with targeted size below 5 µm (preferably below 3 µm) to ensure deep deposition of particles. The final critical attribute was focused on the delivery of iron oxide particles along with dactinomycin which would enable targeting of the particles using a magnetic field (such as magnetic resonance imaging – MRI).

Several formulations were developed, and initial results demonstrated effective deposition of the nanoaggregate onto the NGI trays as depicted in **Fig. 2**. Slight variation in API concentration and polymer concentration showed differences in DPI performance and hence were to be included

in the QbD study. Because all batches demonstrated excellent content uniformity (97.78%-101.54%) of the powder, content uniformity was not included in the QbD study as a CQA.

[Figure 2 near here]

Design of Experiment (DoE)

API concentration, polymer type and polymer concentration in each formulation were selected as the critical input parameters \factors to be included in the DoE study due to their vital roles expected to impact the CQA of the nanoparticles according to initial screening studies, previous studies and compendial requirements. All the parameters were key to successful formulation; however, the best combinations of the polymer type and concentration as well as API concentration to achieve the desirable product performance could not be determined and hence the DoE was initiated. A total of 16 runs were produced by MODDE software, which were prepared and characterised depending on proposed run order. **Table 4** represents the D-optimal design worksheet with the proportions of input parameters, CQA results, and total number of runs as well as the run order. The results were fitted to the MODDE software to enable analysis.

[Table 4 near here]

The fitted data was verified, and outlier experiments were excluded. Overall, the model in this study was verified with total of 13 runs included, 3 outlier runs excluded (N3, N5 and N11) and 7 important model terms identified namely: constant, dactinomycin concentration (API), polymer concentration (PC), polymer type (POL), interactive term (API*PC), quadratic term of drug concentration (API*API), and the interactive term (API*POL).

To validate the model, several plots were investigated. The plot of residues versus run order (**Fig. 3A**) was analysed to indicate if error was built up within the run order. Typically, a good model should demonstrate randomness in run distribution which was clear in our study for all the responses (Eriksson et al. 2000). Additional verification tool was based on determining the observed versus predicted plot (**Fig. 3B**), where the results showed linear correlation with high regression coefficient for all the responses exceeding 0.9, which is an indication of an excellent model.

[Figure 3 near here]

According to the statistical results that were obtained from ANOVA analysis and summarised in **Table 5**, all the regression models were statistically significant for all responses with p value of less than 0.05; while the p value related to the lack of fit was greater than 0.05 as an indication of insignificance.

[Table 5 near here]

Regression Model Equations for CQAs

Upon confirmation of the significance of the CQA terms that were incorporated in the model, the regression model equations for CQAs were determined. The regression model equations for each CQA could be constructed by incorporating only the significance terms. The fitted equations for all CQAs are clarified in Equations. 4-9.

$$Y_1 = 58.18 - 16.29X_1 + 5.51X_3 - 5.51X_4 \quad (4)$$

$$Y_2 = 68.35 - 7.24X_1X_2 - 8.64X_1^2 \quad (5)$$

$$Y_3 = 51.93 + 4.32X_1 + 3.62\,X_2 + 1.86\,X_3 - 1.86\,X_4 - 1.33X_1X_2 + 2.0X_1^2 \quad (6)$$

$$Y_4 = 1.84 + 0.17\,X_1 + 0.13X_2 - 0.11\,X_3 + 0.11X_4 - 0.03X_1X_2 - 0.03X_1X_3 + 0.03X_1X_4 + 0.03\,X_1^2 \quad (7)$$

$$Y_5 = 22.22 + 7.06\,X_1 - 7.62\,X_3 + 7.62\,X_4 - 5.08\,X_1X_3 + 5.08\,X_1X_4 \quad (8)$$

$$Y_6 = 40.10 - 10.30\,X_1 + 5.54\,X_3 - 5.54\,X_4 - 6.17\,X_1X_2 \quad (9)$$

where Y_1 is the emitted dose, Y_2 is the FPF, Y_3 is the EE, Y_4 is the MMAD, Y_5 is the burst effect, and Y_6 is the FPF-Theo. While the main factors were represented in equations as X_1 – API Concentration (%), X_2 – polymer concentration (%), X_3 – polymer type: chitosan; and X_4 – polymer type: Na-alginate. The value of each coefficient represents its impact and the sign (- or +) indicates the positivity or negativity of the effect on the response (Dahmash et al. 2018). For instance, the most significant effect on emitted dose (Y_1) was API concentration (-16.29 X_1) having a vital negative effect on emitted dose. Thus, an increase in API concentration will result in a decrease in emitted dose.

Effect of Critical Input Parameters (Factors) on CQA/Responses

Dactinomycin concentration had a detrimental effect on several responses either as a single factor (**Fig. 4**) or interactive effect (**Fig. 5**). Increasing the API concentration resulted in reduction in the emitted dose and FPF-Theo. Such effect was expected as the high molecular weight API produced denser particles. A similar effect was also noted for MMAD. Higher density of particles results in reduced emitted dose and increased MMAD. Similar trends were observed with research of Patel and co-workers ((2012), where increase in NaCl concentration resulted in higher density particles and hence lower aerodynamic performance of particles. Increase in API concentration also resulted in an increase in EE but that was accompanied by an increase in burst effect. This could be attributed to the increase in dactinomycin particles that are adsorbed to the surface of the nanoparticles and get immediately released in dissolution media (Hussein-Al-Ali et al. 2018).

[Figure 4 near here]

However, when the effect of the interactive term of API concentration and polymer concentration was assessed (as seen in **Fig. 5**), the effect varied. FPF and FPF-Theo were inter-related as both are based on the analysis of dactinomycin quantity from trays 2-7. Therefore, it was expected that the interactive terms would produce similar trends. The Contour plot in **Fig. 5(A)** shows that when the polymer chitosan is used, low API concentration produced low FPF and FPF-Theo at low polymer concentration. However, moving towards intermediate to high polymer concentration resulted in an increase in FPF and FPF-Theo, particularly when the API concentration was set at low to medium range. Maximum performance of the nanoaggregates pertinent to FPF, FPF-Theo and MMAD was observed at low API concentration and medium to high chitosan concentration. Chitosan demonstrates high molecular weight (1526.5 g/mol) (Jana et al. 2013; Adolfo et al. 2017) , which when combined with high API percentage resulted in reduction in the two responses, as expected. Ultimately, increasing API concentration (a high molecular weight drug) will increase the density and hence reduce the flowability and therefore, lower emitted dose, FPF, and FPF- Theo. This was evident also from the increase in MMAD of particles which provides a direct relationship to aerodynamic performance of inhalable particles (Patel et al. 2012).

Fig. 5(A) also revealed the effect of increasing the API and polymer concentrations on entrapment efficiency. Higher polymer and API concentrations for both polymer types resulted in an increase in EE. However, EE showed slightly higher EE level with chitosan than compared to Na-alginate, this is associated with the properties of chitosan which demonstrates higher functional groups on its structure than compared to Na-alginate, therefore increase the possibility of dactinomycin attraction to the polymer (Hill et al. 2019).

[Figure 5 near here]

The aerodynamic properties of the nanoaggregates demonstrated a similar pattern when Na alginate was employed as a polymer. Higher FPF and FPF-Theo were obtained when low to medium concentration of the API was used with medium to high concentration of the polymer. However, the produced particles demonstrated higher MMAD which is proposed to be due to production of denser nanoparticles or presence of larger nanoaggregates (Sheth et al. 2015). When the produced formulations were examined, it was noted that for most formulations the MMAD did not exceed 2 µm which is a favourable size. However, higher MMAD is based on larger nanoaggregates that produced higher density which jeopardised emitted dose, FPF and FPF-Theo.

Burst Effect

The primary reason for the selection of this response/ CQA was to develop formulations where the release of the API could be delayed. This would ensure that dactinomycin is not released until it reaches the lower part of the respiratory system. Hence, a low burst effect is favourable and thus a critical quality attribute. Equation 8 reveals the effect of polymer type on burst effect. While increasing the concentration of chitosan resulted in reduction in the burst effect, increasing the concentration of Na-alginate resulted in an increase in the burst effect. The effect of API concentration and polymer type on the burst effect revealed a positive effect of the interaction term when chitosan is used by reducing the burst effect while a negative outcome is demonstrated when Na-alginate is used. At low API concentration chitosan demonstrated better protection of the formulation as demonstrated by low burst effect. However, increasing the API concentration of both polymers affected the burst effect negatively with chitosan showing a superior effect (more protection i.e., less release within first 10 minutes) (see **Fig. 6**). Reports of few studies revealed the poor encapsulation efficiency and high burst effect of Na-alginate nanoparticles (Rahaiee et al. 2017; Choukaife et al. 2020). The proposed reason for this was the hydrophilicity and porosity of

alginate- nanoparticles that contributed to increased instability, leakage of the entrapped drug and swelling upon hydration (Lee and Mooney 2012; Hasnain and Nayak 2019).

[Figure 6 near here]

Prediction of Design Space

Employing all of the results that were obtained from significant individual and interactive effects on CQA within the study, the sweet plot was used to determine the optimal area in which all the results of the responses were within the desired range limits of FPF (30-60%), emitted dose >60% up to 90%, EE within the range (40-70%), MMAD less than 3 µm and larger than 1 µm; plus burst effect and FPF-Theo within the range (0-20%) and (30-60%) respectively. From the sweet spot plot (**Fig. 7**), the green area denotes the design space in which all the responses results were within the targeted values. While other colours represent areas in which factors would meet the specification of five responses or less. As shown in **Fig. 7A**, when a concentration of API is between 2.1% to 2.5% with polymer concentration ranging from 0.5% to 0.9% using chitosan; or concentration of API is between 2% to 2.54% with polymer concentration ranging from 0.5% to 1.3% using Na alginate; the desired target outcomes would be achieved.

[Figure 7 near here]

Representative formulations as can be seen in **Fig. 7** are marked with arrow 1-4. Formulation parameters and corresponding CQA are presented in **Table 6**. As can be seen from the table, chitosan polymer showed superiority in terms of burst effect and MMAD. Therefore, owing to this

property, the chitosan containing formulation was selected for further characterisation to develop a better understanding of the molecular and surface profile of the nanoparticles.

[Table 6 near here]

Characterisation and Molecular Profiling of Dactinomycin -Chitosan-IONP

The DSC thermogram of chitosan showed a wide endothermic peak that resolved at a value of 74.55 °C and peak temperature of 93.77 °C (**Fig. 8A**). Chitosan is a biopolymer and high thermal energy is required for the dissociation of its structure (Ramasamy et al. 2014). Chitosan-IONP showed a wider peak at a slightly lower temperature (91.12 °C) with lower enthalpy of 4.66 J/g vs 13.5 J/g for chitosan alone (**Fig. 8B**). A study by Carp et al. (2010), reported that polymers adsorbed on iron oxide nanoparticles surface decompose at lower temperatures than free polymers, which is attributed to the catalytic effect of iron oxide towards the degradation of the organic coating. Furthermore, **Fig. 8C** represents the DSC of dactinomycin-chitosan-IONP that showed a wider endothermic peak starting at 92.4 ºC which represents the chitosan component. Dactinomycin melting was between 245 and 248 ºC which started to appear at 250 ºC as can be seen from the thermogram.

[Figure 8 near here]

Fig. 9 shows the TEM images of dactinomycin-chitosan-IONPs. The TEM images (**Fig. 9 A-B**) represent spherical and/or irregular morphology of iron oxide NPs. The TEM also revealed that the nanoparticles were present as nanoaggregates, which is a key attribute for effective pulmonary drug delivery. The particles showed a narrow size distribution (**Fig. 9-C**) with an average size of 4.4 ± 0.77 nm (n=32).

[Figure 9 near here]

Further investigation of the composition of the nanoparticles was made using SEM-EDS analysis. As shown in **Fig. 10**, only iron and oxygen elements existed in the IONP (**Fig. 10A**) with a Fe/O atomic ratio of about 3:3.97 which is consistent with the theoretical value of Fe_3O_4. No other elements could be detected, indicating the high purity of the IONP nanoparticles. **Fig. 10B** revealed the presence of nitrogen, oxygen and carbon which are the elemental components of chitosan powder. **Fig. 10C** demonstrated the presence of iron, oxygen, carbon, and nitrogen indicating the presence of both chitosan and iron oxide within the particles. **Fig. 10D** shows the elemental composition of IONP-chitosan and dactinomycin.

[Figure 10 near here]

The final set of analysis was based on XRD. **Fig. 11** shows the X-ray diffraction patterns for dactinomycin (**Fig. 11A**), IONP (**Fig. 11B**) and the dactinomycin- chitosan- IONP (Fig. 11C). Dactinomycin is present as a crystalline material despite the shortage of sharp peaks. The IONP showed clear characteristic peaks at 30.4 º, 35.5 º, 43.5º, 57.3 º and 62.9º which correspond to magnetite (Fe_3O_4). Similar results were reported for magnetite highlighting the presence of magnetic nanoparticles (Hussein-Al-Ali et al. 2014). The XRD pattern of dactinomycin-chitosan-IONP contained the same characteristic peaks of the IONP without any shift in the peaks, however, the peaks showed lower intensity which is due to the presence of dactinomycin within the particles. It was also noted that the a disappearance of the characteristic peaks of dactinomycin which could be attributed to the drug being dissolved within the polymeric chains and attracted to the particles through hydrogen bonding. Such results are confirmed with the low burst effect of most chitosan containing formulation that did not exceed 20% supporting that the drug was encapsulated within the nanoparticles, and little was attached to the nanoparticle surface.

[Figure 11 near here]

The molecular profiling analysis demonstrated the successful development of targeted nanoparticles with chitosan polymer. Such particles developed an effective dry powder inhalation formulation.

Conclusions

The current study describes a strategy for formulating dry powder inhalers (DPI) for targeted drug delivery to the respiratory system. This work employed a quality by design (QbD) approach, utilising design of experiments (DoE) to develop iron oxide nanoparticles for the delivery of dactinomycin, a model anticancer drug, to the lungs. Dactinomycin, at three different doses, was selected as model API: with chitosan and Na alginate as polymers also with three different concentrations. DPIs with desired target properties in terms of FPF, EE, MMAD, FPF-Theo, burst effect and emitted dose were successfully developed. Results showed chitosan IONPs as superior to those containing Na alginate. Also, maintaining dactinomycin concentration at 2.1 – 2.5% and chitosan concentration at 0.5 - 0.9% produced optimal IONPs. The novelty in this project stems from using iron oxide nanoparticles loaded with the drug in DPI formulation targeted directly to the lung, avoiding the burst effect phenomenon. The complexity of this project lies in the challenges encountered in handling dactinomycin pertinent to its heat and light instability as well as high molecular weight. Further studies will investigate the toxicity profile of these iron oxide nanoparticles *in vitro* on pulmonary cell cultures and *in vivo* using animal models.

Acknowledgements

Isra University (Jordan) provided funding for Dr. Eman Dahmash and Dr. Samir Al Ali (grant 50/3/2018-2019). Najran University and Aston University provided financial support to Dr. Hamad Alyami and Dr. Affiong Iyire respectively, to work on this project.

Declaration of Competing Interest

The authors declare that they have no known competing financial interests or personal relationships that could have appeared to influence the work reported in this paper.

Authors Contributions S.F.A., S.M.A., S.H.A and H.S.A conducted the research. E.Z.D conceived, supervised the project, conducted the research and wrote the manuscript. A.I. revised and updated the manuscript. All authors reviewed the manuscript.

References

Acharya G, Mitra AK, Cholkar K. 2017. Nanosystems for Diagnostic Imaging, Biodetectors, and Biosensors. In: Mitra, Ashim K.; Cholkar KM, Abhirup, editors. Emerg Nanotechnologies Diagnostics, Drug Deliv Med Devices. 1st ed. Collegeville, PA, United States: Elsevier; p. 217–248. https://doi.org/10.1016/B978-0-323-42978-8.00010-3

Adolfo G, Ruiz M, Fabio H, Fabio H, Corrales Z. 2017. Chitosan, chitosan derivatives and their biomedical applications. In: Shalaby E, editor. Biol Act Appl Mar polysaccharides. 1st editio. Croatia; p. 87–104.

Bhattacharjee S. 2020. Understanding the burst release phenomenon: toward designing effective nanoparticulate drug-delivery systems. Ther Deliv [Internet]. 12(1):21–36. https://doi.org/10.4155/tde-2020-0099

Carp O, Patron L, Culita D, Budrugeac P, Feder M, Diamandescu L. 2010. Thermal analysis of two types of dextran-coated magnetite. J Therm Anal Calorim. 101(1):181–187.

Choukaife H, Doolaanea AA, Alfatama M. 2020. Alginate Nanoformulation: Influence of Process and Selected Variables. Pharmaceuticals. 13(11):335.

Dahmash EZ, Al-Khattawi A, Iyire A, Al-Yami H, Dennison TJ, Mohammed AR. 2018. Quality by Design (QbD) based process optimisation to develop functionalised particles with modified release properties using novel dry particle coating technique. PLoS One. 13(11):e0206651.

Eriksson L, Johansson E, Kettaneh-Wold N, Wikström C, Wold S. 2000. Design of experiments. Princ Appl Learn ways AB, Stock.

Gokduman K, Bestepe F, Li L, Yarmush ML, Usta OB. 2018. Dose-, treatment- A nd time-dependent toxicity of superparamagnetic iron oxide nanoparticles on primary rat hepatocytes. Nanomedicine. 13(11):1267–1284. https://doi.org/10.2217/nnm-2017-0387

Gwaltney-Brant SM. 2010. Antineoplastic Drugs. Seventh Ed. [place unknown]: Elsevier. https://doi.org/10.1016/B978-0-08-046884-6.00852-6

Han G, Ghosh P, Rotello VM. 2007. for Drug Delivery. Science (80-).(August):18–26. https://doi.org/10.1016/B978-0-323-46143-6/00030-0

Hanini A, Schmitt A, Kacem K, Chau F, Ammar S, Gavard J. 2011. Evaluation of iron oxide nanoparticle biocompatibility. Int J Nanomedicine. 6:787–94. https://doi.org/10.2147/IJN.S17574

Haschek WM, Bolon B, Rousseaux CG, Wallig MA. 2010. Fundamentals of Toxicologic Pathology. [place unknown].

Hasnain MS, Nayak AK. 2019. Alginates: versatile polymers in biomedical applications and therapeutics. [place unknown]: CRC Press.

577 Hill M, Twigg M, Sheridan EA, Hardy JG, Elborn JS, Taggart CC, Scott CJ, Migaud ME. 2019. Alginate/chitosan
578 particle-based drug delivery systems for pulmonary applications. Pharmaceutics. 11(8).
579 https://doi.org/10.3390/pharmaceutics11080379

580 Hussein-Al-Ali SH, Kura A, Hussein MZ, Fakurazi S. 2018. Preparation of chitosan nanoparticles as a drug delivery
581 system for perindopril erbumine. Polym Compos [Internet]. 39(2):544–552.
582 https://doi.org/https://doi.org/10.1002/pc.23967

583 Hussein-Al-Ali SH, El Zowalaty ME, Hussein MZ, Ismail M, Webster TJ. 2014. Synthesis, characterization,
584 controlled release, and antibacterial studies of a novel streptomycin chitosan magnetic nanoantibiotic. Int J
585 Nanomedicine [Internet]. 9:549–557. https://doi.org/10.2147/IJN.S53079

586 ICH. 2005. Validation of analytical procedures: Text and methodology Q2(R1). Int Conf Harmon Tech Requir
587 Regist Pharm Hum Use. 4.

588 Jana S, Maji N, Nayak AK, Sen KK, Basu SK. 2013. Development of chitosan-based nanoparticles through inter-
589 polymeric complexation for oral drug delivery. Carbohydr Polym. 98(1):870–876.
590 https://doi.org/10.1016/j.carbpol.2013.06.064

591 Jana Sougata, Jana Subrata. 2016. Natural polymeric biodegradable nanoblend for macromolecules delivery. [place
592 unknown]: Elsevier Ltd. https://doi.org/10.1016/B978-0-08-100408-1.00010-8

593 Kammari R, Das NG, Das SK. 2017. Nanoparticulate Systems for Therapeutic and Diagnostic Applications. [place
594 unknown]: Elsevier. https://doi.org/10.1016/B978-0-323-42978-8.00006-1

595 Kaur A, Katiyar SS, Kushwah V, Jain S. 2017. Nanoemulsion loaded gel for topical co-delivery of clobitasol
596 propionate and calcipotriol in psoriasis. Nanomedicine Nanotechnology, Biol Med. 13(4):1473–1482.
597 https://doi.org/10.1016/j.nano.2017.02.009

598 Kulkarni VS. 2009. Handbook of non-invasive drug delivery systems : science and technology. [place unknown]:
599 William Andrew.

600 Lee KY, Mooney DJ. 2012. Alginate: properties and biomedical applications. Prog Polym Sci. 37(1):106–126.

601 Liang Z, Ni R, Zhou J, Mao S. 2015. Recent advances in controlled pulmonary drug delivery. Drug Discov Today
602 [Internet]. 20(3):380–389. https://doi.org/10.1016/j.drudis.2014.09.020

603 Maiti S, Kumari L. 2016. Smart Nanopolysaccharides for the Delivery of Bioactives. [place unknown]: Elsevier Inc.
604 https://doi.org/10.1016/B978-0-323-47347-7.00003-3

605 McMillan J, Batrakova E, Gendelman HE. 2011. Cell delivery of therapeutic nanoparticles. 1st ed. [place unknown]:
606 Elsevier Inc. https://doi.org/10.1016/B978-0-12-416020-0.00014-0

607 Muthuraman A, Kaur J. 2017. Antimicrobial Nanostructures for Neurodegenerative Infections: Present and Future

608 Perspectives. [place unknown]: Elsevier Inc. https://doi.org/10.1016/B978-0-323-46152-8.00006-8

609 Patel B, Gupta V, Ahsan F. 2012. PEG–PLGA based large porous particles for pulmonary delivery of a highly
610 soluble drug, low molecular weight heparin. J Control Release. 162(2):310–320.
611 https://doi.org/https://doi.org/10.1016/j.jconrel.2012.07.003

612 Rahaiee S, Hashemi M, Shojaosadati SA, Moini S, Razavi SH. 2017. Nanoparticles based on crocin loaded
613 chitosan-alginate biopolymers: Antioxidant activities, bioavailability and anticancer properties. Int J Biol Macromol.
614 99:401–408.

615 Ramasamy P, Subhapradha N, Shanmugam V, Shanmugam A. 2014. Extraction, characterization and antioxidant
616 property of chitosan from cuttlebone Sepia kobiensis (Hoyle 1885). Int J Biol Macromol. 64:202–212.

617 Rozet E, Lebrun P, Michiels J-F, Sondag P, Scherder T, Boulanger B. 2015. Analytical Procedure Validation and
618 the Quality by Design Paradigm. J Biopharm Stat. 25(2):260–268. https://doi.org/10.1080/10543406.2014.971176

619 Sheth P, Stein SW, Myrdal PB. 2015. Factors influencing aerodynamic particle size distribution of suspension
620 pressurized metered dose inhalers. AAPS PharmSciTech [Internet]. 16(1):192–201. https://doi.org/10.1208/s12249-
621 014-0210-z

622 Singh N, Joshi A, Toor AP, Verma G. 2017. Drug delivery: advancements and challenges. [place unknown]:
623 Elsevier Inc. https://doi.org/10.1016/b978-0-323-46143-6.00027-0

624 USP-31. 2008. 601 Aerosols, nasal sprays, metered-dose inhalers, and dry powder inhalers. United States
625 Pharmacopea.

626 USP-35. 2011. The United States pharmacopeia : the National Formulary : USP 35 NF 30th Edition. Authority of
627 the United States Pharmacopeial Convention I, editor. Washington, D.C. Rockville: USP, C. (2011). The United
628 States Pharmacopeia. National Formulary.

629 Wang M, Marepally SK, Vemula PK, Xu C. 2016. Inorganic Nanoparticles for Transdermal Drug Delivery and
630 Topical Application. Nanosci Dermatology.:57–72. https://doi.org/10.1016/B978-0-12-802926-8.00005-7

631 Wang Y, Ding L, Yao C, Li C, Xing X, Huang Y, Gu T, Wu M. 2017. Toxic effects of metal oxide nanoparticles
632 and their underlying mechanisms. Sci China Mater. 60(2):93–108. https://doi.org/10.1007/s40843-016-5157-0

633 Zimmermann CM, Baldassi D, Chan K, Adams NBP, Neumann A, Porras-Gonzalez DL, Wei X, Kneidinger N,
634 Stoleriu MG, Burgstaller G. 2022. Spray drying siRNA-lipid nanoparticles for dry powder pulmonary delivery. J
635 Control Release. 351:137–150.

636

637

638 **Table 1** List of factors and CQA/ responses with their details that were used in DoE.

Name	Abbr.	Units	Type	Settings		
				Low	Middle	High
Factors						
API-Conc	API	%	Multilevel	2	3.5	5
Polymer type	Pol	-	Qualitative	Chitosan, Na-Alginate		
Pol-Conc	PC	%	Quantitative	-1*	0*	1*
CQA/ Responses						
Name	**Abbr.**	**Units**	**Transform**	**Min**	**Target**	**Max**
FPF	FPF	%	None	10	30	50
Emitted dose	ED	%	None	50	70	90
Entrapment Efficiency	EE	%	None	30	50	70
MMAD	MMA	micron	None	1	2	5
Burst Effect	BE	%	None	0	10	30
FPF-Theoretical	FPT	%	None	10	25	40

***Concentrations of polymers used were as follows: -1 (low): 0.5%, 0 (medium): 1%, 1 (high): 2%**

639

640

641 **Table 2** Worksheet of experiments that were generated by MODDE Software

Exp No	Exp Code	Run Order	Incl/ Excl*	API-Conc	Polymer type	Pol-Con
1	N1	3	Incl	2	Chitosan	-1
2	N2	6	Incl	2	Chitosan	1
3	N3	11	Incl	2	Chitosan	0
4	N4	4	Incl	3.5	Chitosan	-1
5	N5	2	Incl	3.5	Chitosan	1
6	N6	5	Incl	5	Chitosan	-1
7	N7	8	Incl	5	Chitosan	1
8	N8	9	Incl	5	Chitosan	0
9	N9	16	Incl	2	Na-Alginate	-1
10	N10	14	Incl	2	Na-Alginate	1
11	N11	15	Incl	3.5	Na-Alginate	0
12	N12	13	Incl	5	Na-Alginate	-1
13	N13	12	Incl	5	Na-Alginate	1
14	N14	1	Incl	3.5	Na-Alginate	0
15	N15	7	Incl	3.5	Na-Alginate	0
16	N16	10	Incl	3.5	Na-Alginate	0

642 *Incl/Excl is included or excluded run

643

644 **Table 3** Intermediate precision and reproducibility of HPLC method of dactinomycin, to evaluate inter and intraday
645 reproducibility

Dactinomycin Theoretical Concentration (µg/mL)	Intraday % Recovery (mean ± SD) (n=3)	Intraday %RSD (n=3)	Interday % Recovery (mean ± SD) (n=9)	Interday %RSD (n=9)
1000	99.92 ± 0.90	0.90	99.94 ± 0.65	0.66
500	100.32 ± 0.90	0.90	100.02 ± 0.81	0.81
250	100.09 ± 1.92	1.92	99.89 ± 1.71	1.72
125	99.43 ± 1.56	1.57	99.21 ± 1.40	1.41
62.5	99.60 ± 1.34	1.35	99.59 ± 1.20	1.21
31.75	97.90 ± 2.05	2.09	97.94 ± 1.83	1.87
15.625	99.79 ± 2.50	2.51	99.19 ± 2.89	2.91

646

647

Table 4 The D-optimal design worksheet with the proportions of factors, CQA results, the total number of runs as well as the run order

Exp No	Exp Name	Run Order	Incl/ Excl	API-Conc %w/w	Polymer type	Pol-Con %w/w	FPF %	Emitted dose %	EE %	MMAD µm	Burst Effect %	FPF-Theo %
1	N1	3	Incl	2	Chitosan	-1	48.61	91.02	46.23	1.5	14.4	44.25
2	N2	6	Incl	2	Chitosan	1	79.64	82.15	59.65	1.71	8	65.42
3	N3	11	Excl	2	Chitosan	0	42.92	87.34	58.1	1.45	11.6	37.49
4	N4	4	Incl	3.5	Chitosan	-1	67.48	75.5	50.01	1.62	11.35	50.95
5	N5	2	Excl	3.5	Chitosan	1	60.06	65.78	60.16	1.93	10.43	39.51
6	N6	5	Incl	5	Chitosan	-1	63.95	63.43	56.43	1.71	20	40.56
7	N7	8	Incl	5	Chitosan	1	48.27	48.54	63.43	2.12	15	23.43
8	N8	9	Incl	5	Chitosan	0	62.2	58.98	61.02	1.94	18	36.69
9	N9	16	Incl	2	Na-Alginate	-1	44.38	89.95	42.12	1.65	18.08	39.92
10	N10	14	Incl	2	Na-Alginate	1	63.68	93.25	53.21	1.9	12.23	59.38
11	N11	15	Excl	3.5	Na-Alginate	0	59.8	53.43	60.01	1.93	32.02	31.95
12	N12	13	Incl	5	Na-Alginate	-1	56.19	46.64	55.54	2.02	45.32	26.21
13	N13	12	Incl	5	Na-Alginate	1	48.62	37.91	60.1	2.41	35.08	18.43
14	N14	1	Incl	3.5	Na-Alginate	0	69.23	48.34	48.43	1.93	29.67	33.47
15	N15	7	Incl	3.5	Na-Alginate	0	67.49	56.95	51.23	1.91	26.69	38.44
16	N16	10	Incl	3.5	Na-Alginate	0	64.13	49.65	50.98	1.94	30	31.84

652 **Table 5** Summary of results obtained from ANOVA. R^2 is the goodness of fit of each response

Response	P- value		R^2
	Regression	Lack to fit	
Burst effect	0.001	0.192	0.953
Emitted dose	0.002	0.311	0.943
FPF	0.006	0.226	0.913
EE	0.000	0.730	0.979
MMAD	0.000	0.181	0.993
FPF- Theo	0.001	0.369	0.948

653

654

655 **Table 6** Representative formulations that will fulfil the design space requirements for all the 6 CQA

Parameter	Formulation			
	1	2	3	4
	Factors (Process Parameters)			
API conc. (%)	2.07	2.59	2.0	2.54
Pol conc. (%)	0.9	0.5	1.3	0.9
Polymer type	Chitosan	Chitosan	Na-alginate	Na-alginate
	Responses (CQA)			
FPF (%)	59.7	59.79	59.93	59.91
ED (%)	89.8	81.46	86.68	74.23
EE (%)	50.89	47.06	49.95	46.84
MMAD (µm)	1.59	1.52	1.80	1.79
BE (%)	12.79	15.29	13.64	19.9
FPF-Theo (%)	53.11	46.46	51.55	42.85

656

Figure Captions:

Figure 1. Dactinomycin chemical structure

Figure 2. Deposition of the nanoaggregates onto the NGI apparatus highlighting the dark brown powder collected from tray 1-7 and the MOC which represents the dactinomycin – chitosan -IONP

Figure 3. Model validation plots **(A)** the residual versus run order plot shows a well randomness of run distribution which in turn indicates a good model **(B)**The observed versus predicted plots of all responses that show linearity correlation of emitted dose, MMAD, burst effect, FFP, FPF-Theo and IFPF which corresponding with good model

Figure 4. Main effect of increasing dactinomycin concentration (API-Conc.) on responses (MMAD, EE%, Emitted dose, Burst effect and FPF-Theo)

Figure 5. Response Contour Plot highlighting the interactive effect of API concentration and polymer concentration on responses when **(A)** chitosan was the selected polymer and **(B)** Na- alginate was the selected polymer

Figure 6. Interaction plot of the interactive effect of API concentration and polymer type on burst effect

Figure 7. The sweet spot for optimal proportion of factors (API concentration, polymer type (chitosan), polymer concentration) to obtain the desired responses relating to FPF (30-60%), emitted dose (60-90%), EE (40-70%), MMAD (1-3 µm), burst effect (0-20%) and FPF-Theo (30-60%). (A) The polymer is chitosan (B) The polymer is Na-alginate. Arrows 1-4 represent sample sweet spots where all criteria are met

Figure 8. DSC thermogram of (A) chitosan Powder (B) chitosan with IONP (C) dactinomycin- chitosan- IONP

Figure 9. TEM images of the dactinomycin – chitosan- IONP using various magnifications and highlighting the presence of nanoaggregates (A – B), particle size distribution (C)

Figure 10. SEM–EDS elemental analysis of (A) IONP, (B) chitosan powder, (C) IONP coated with chitosan (D) dactinomycin- chitosan- IONP highlighting the presence of iron and oxygen elements within the nanoparticles

Figure 11. Powder XRD patterns of dactinomycin (A), chitosan-IONP (B), and dactinomycin- chitosan-IONP (C), au: arbitrary unit

Figure 1

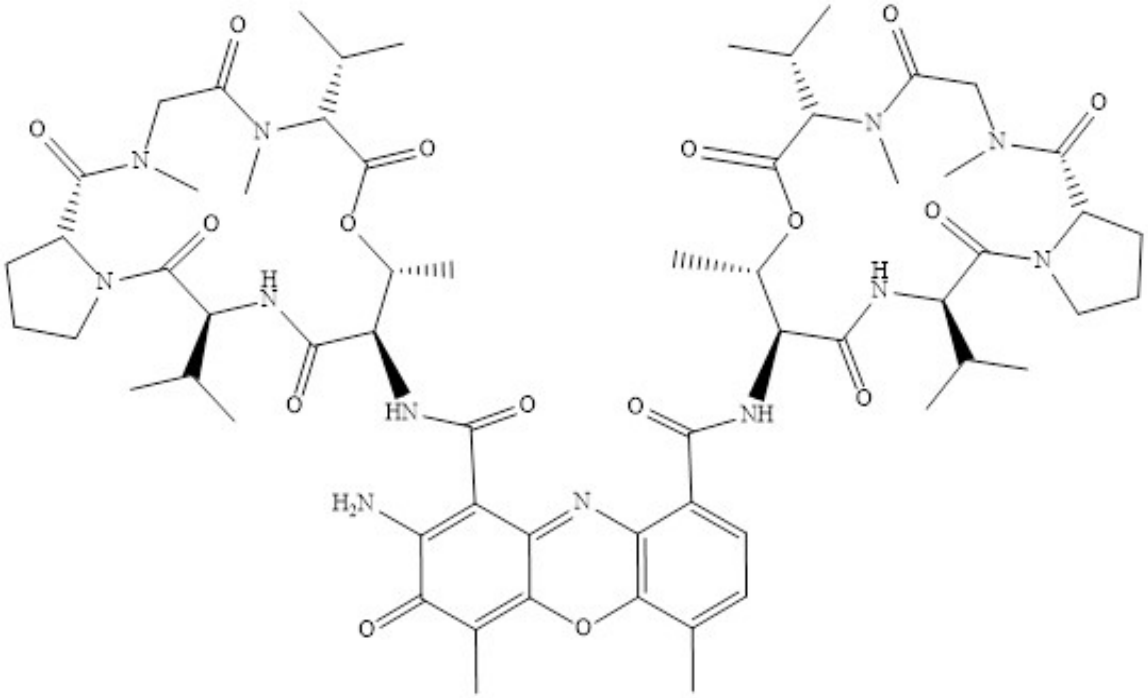

688 **Figure 2**

689

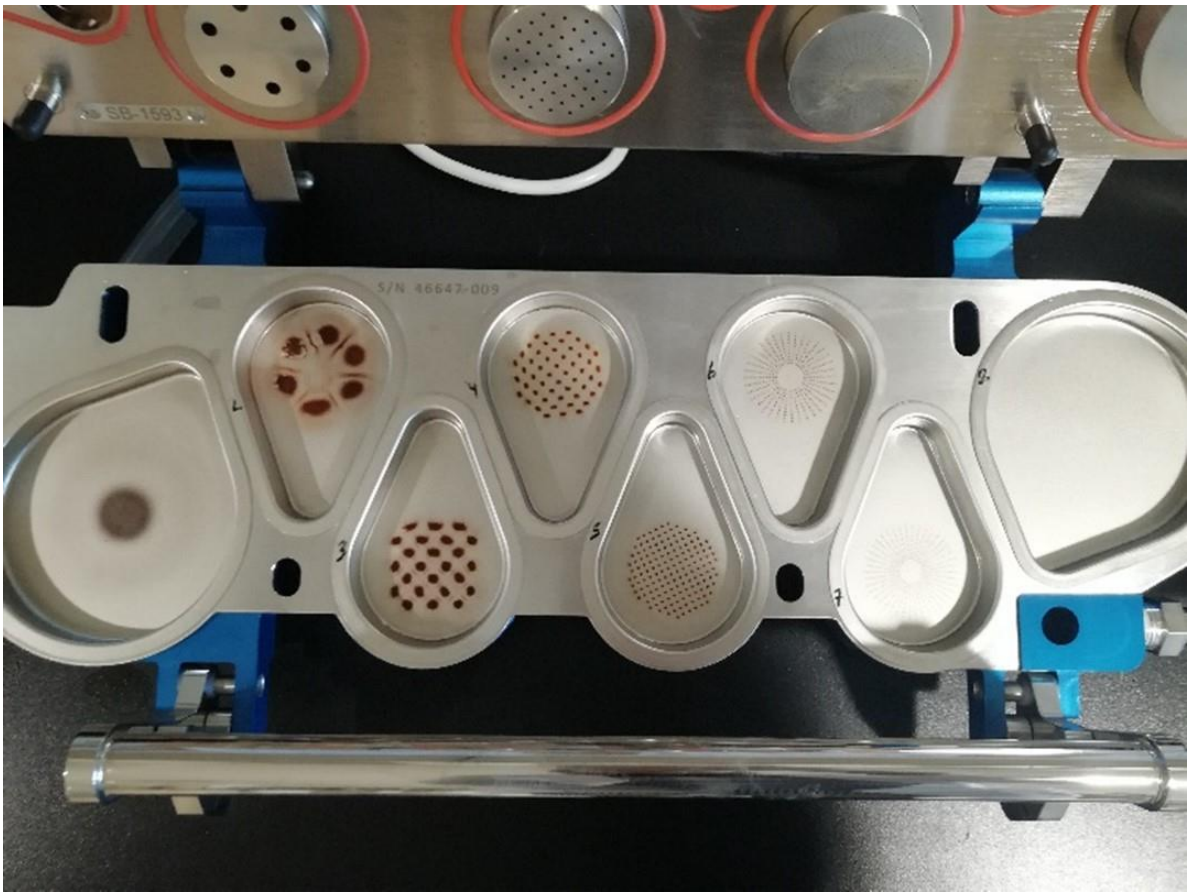

690

691

692

Figure 3

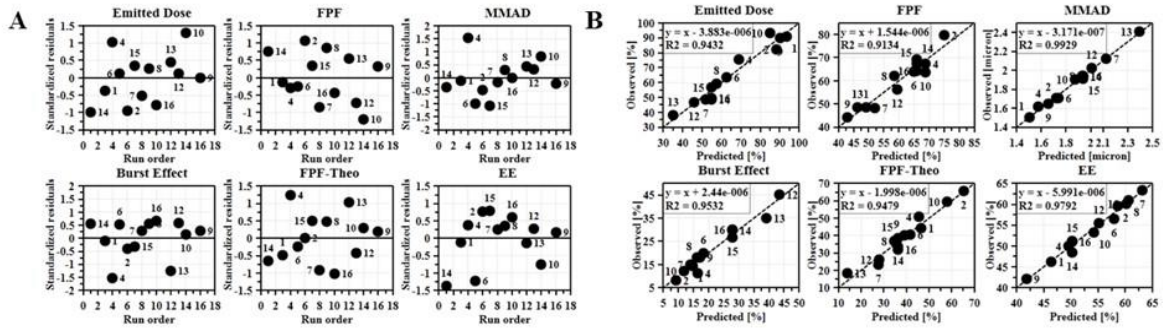
A
Emitted Dose
FPF
MMAD
Burst Effect
FPF-Theo
EE
Standardized residuals
Run order
B
Emitted Dose
y = x - 3.853e-006
R2 = 0.9432
FPF
y = x + 1.544e-006
R2 = 0.9134
MMAD
y = x - 3.171e-007
R2 = 0.9929
Burst Effect
y = x + 2.44e-006
R2 = 0.9532
FPF-Theo
y = x - 1.998e-006
R2 = 0.9479
EE
y = x - 5.991e-006
R2 = 0.9792
Observed [%]
Predicted [%]
Observed [micron]
Predicted [micron]

Figure 4

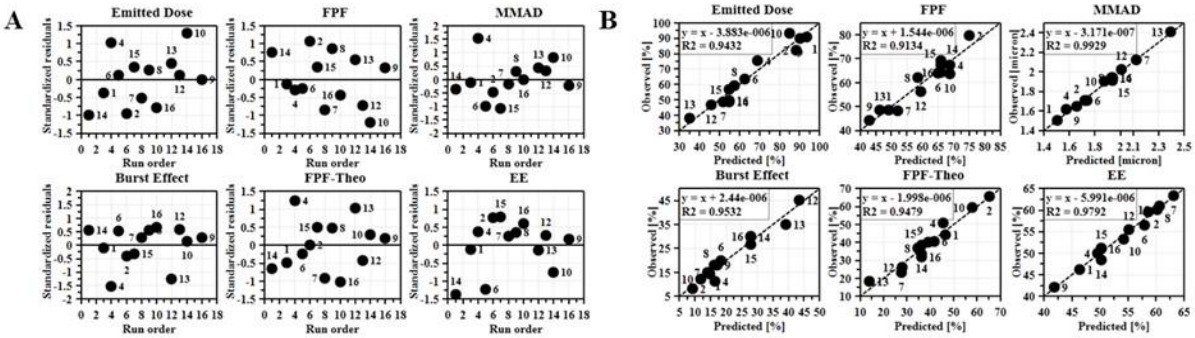
A
Emitted Dose
FPF
MMAD
Burst Effect
FPF-Theo
EE
Standardized residuals
Run order
B
Emitted Dose
y = x - 3.883e-006
R2 = 0.9432
FPF
y = x + 1.544e-006
R2 = 0.9134
MMAD
y = x - 3.171e-007
R2 = 0.9929
Burst Effect
y = x + 2.44e-006
R2 = 0.9532
FPF-Theo
y = x - 1.998e-006
R2 = 0.9479
EE
y = x - 5.991e-006
R2 = 0.9792
Observed [%]
Observed [micron]
Predicted [%]
Predicted [micron]

Figure 5

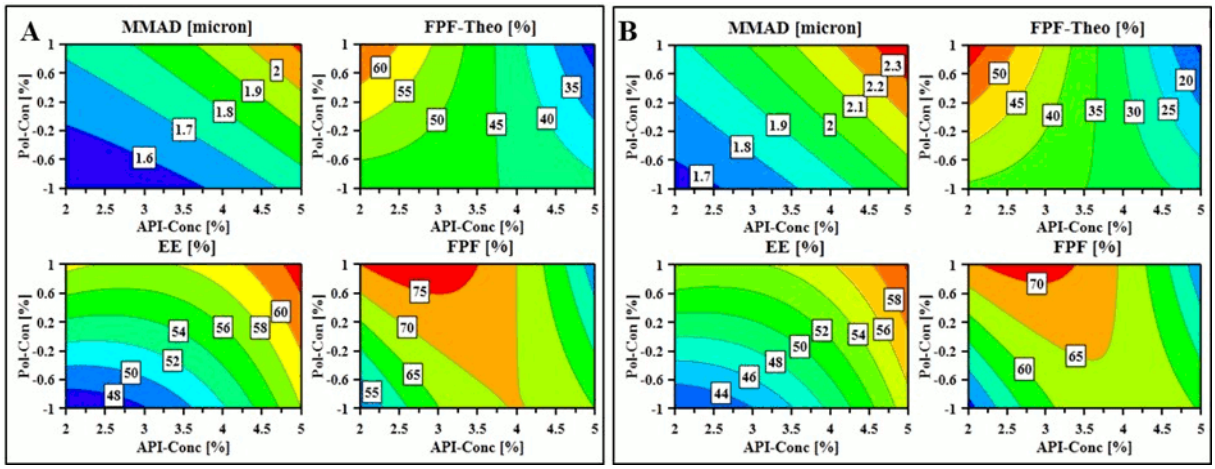
A
MMAD [micron]
FPF-Theo [%]
EE [%]
FPF [%]
Pol-Con [%]
API-Conc [%]
B
MMAD [micron]
FPF-Theo [%]
EE [%]
FPF [%]
Pol-Con [%]
API-Conc [%]

705 **Figure 6**

706

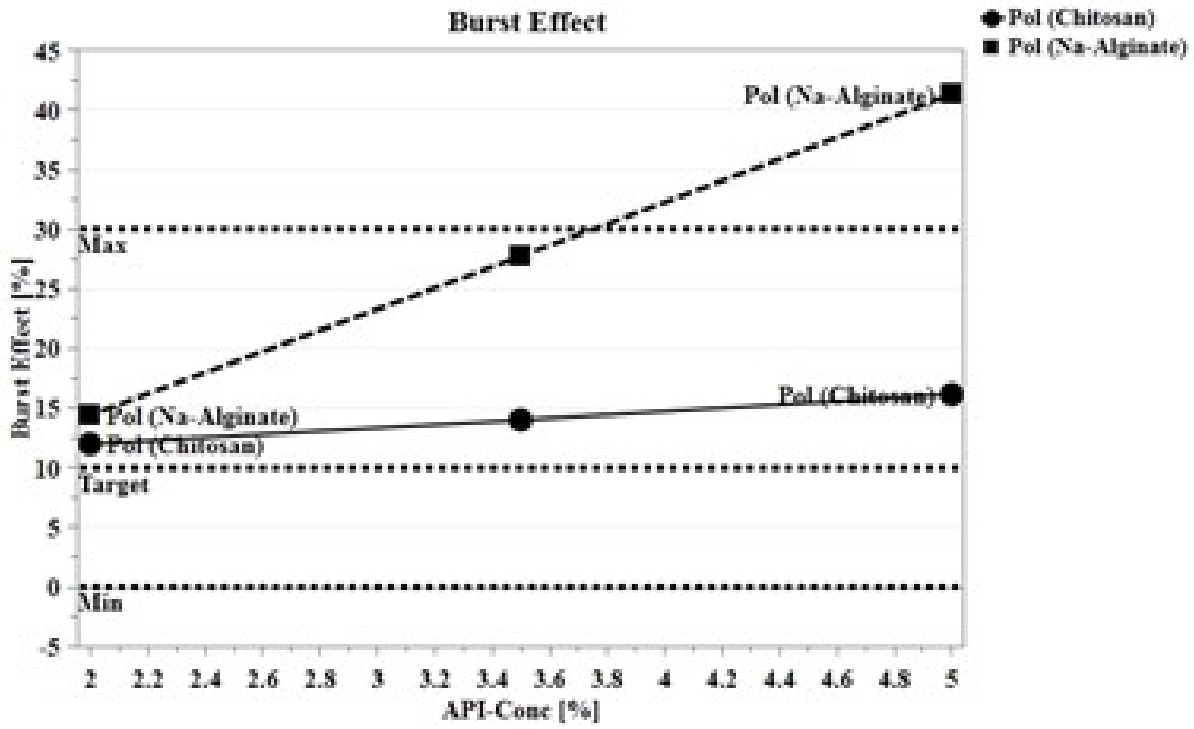

707

708

Figure 7

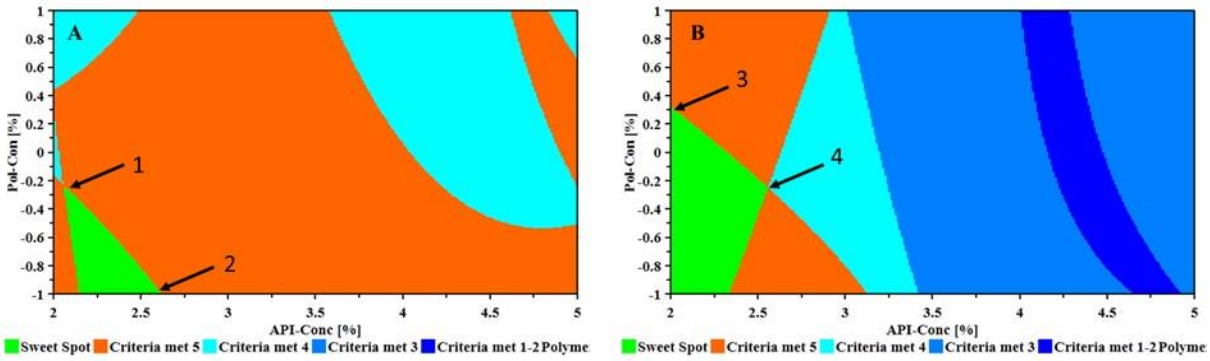
A
B
1
2
3
4
Pot-Con [%]
API-Conc [%]
Sweet Spot
Criteria met 5
Criteria met 4
Criteria met 3
Criteria met 1-2
Polyme

713 **Figure 8**

714

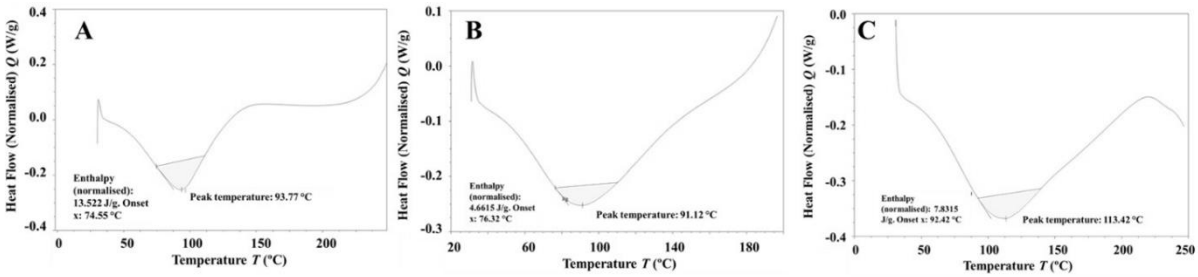

715

716

717 **Figure 9**

718

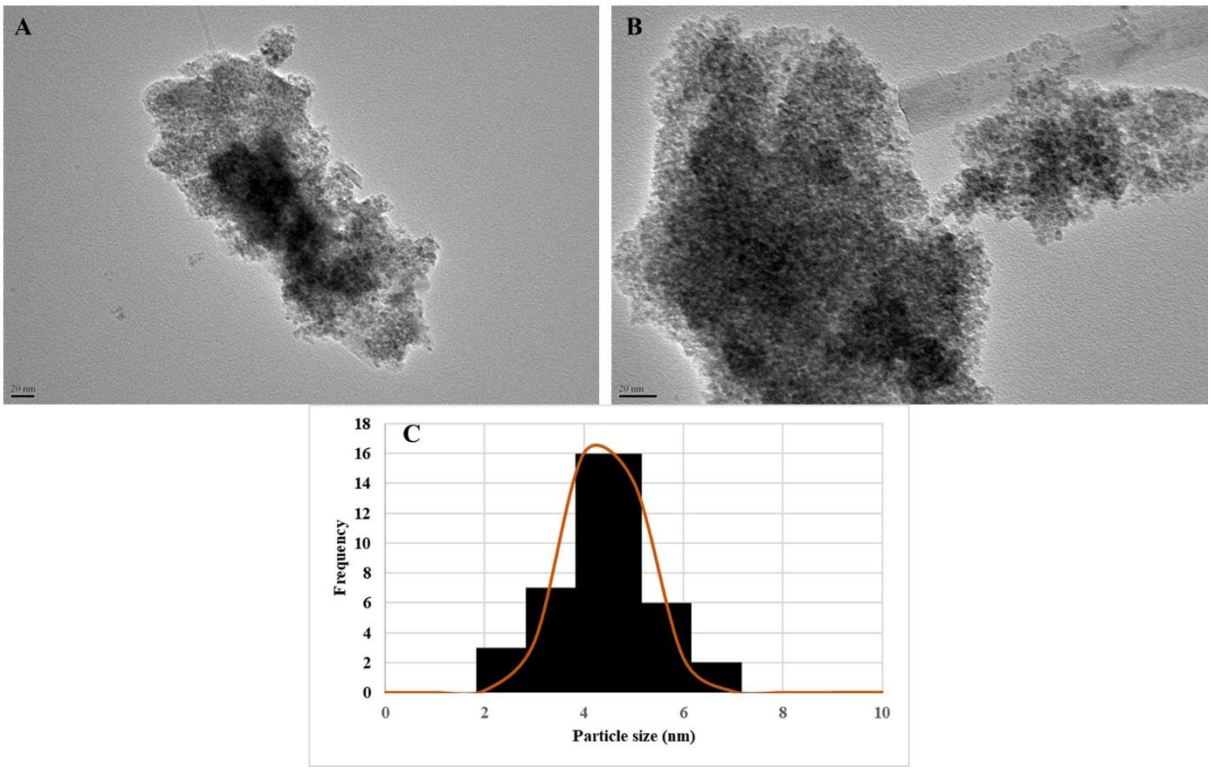

719

720

Figure 10

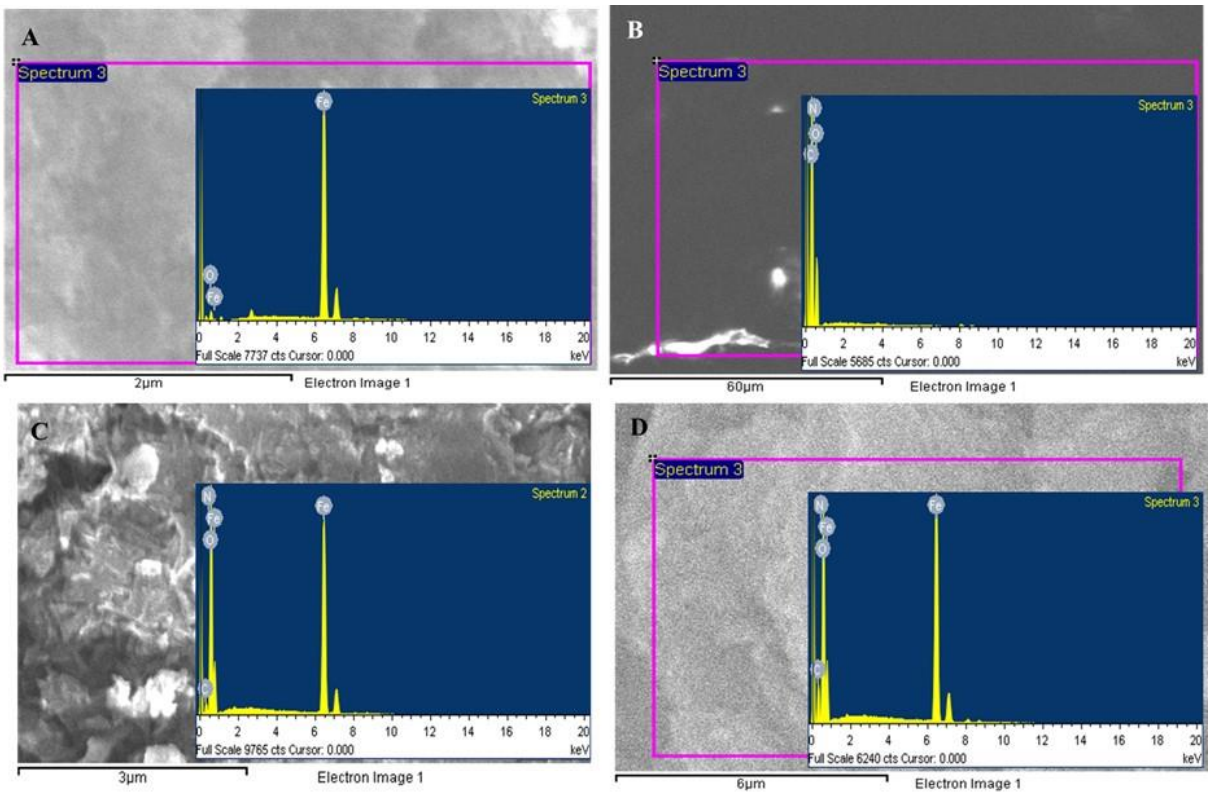
A
Spectrum 3
Spectrum 3
Full Scale 7737 cts Cursor: 0.000
keV
2µm
Electron Image 1
B
Spectrum 3
Spectrum 3
Full Scale 5685 cts Cursor: 0.000
keV
60µm
Electron Image 1
C
Spectrum 2
Full Scale 9765 cts Cursor: 0.000
keV
3µm
Electron Image 1
D
Spectrum 3
Spectrum 3
Full Scale 6240 cts Cursor: 0.000
keV
6µm
Electron Image 1

Figure 11

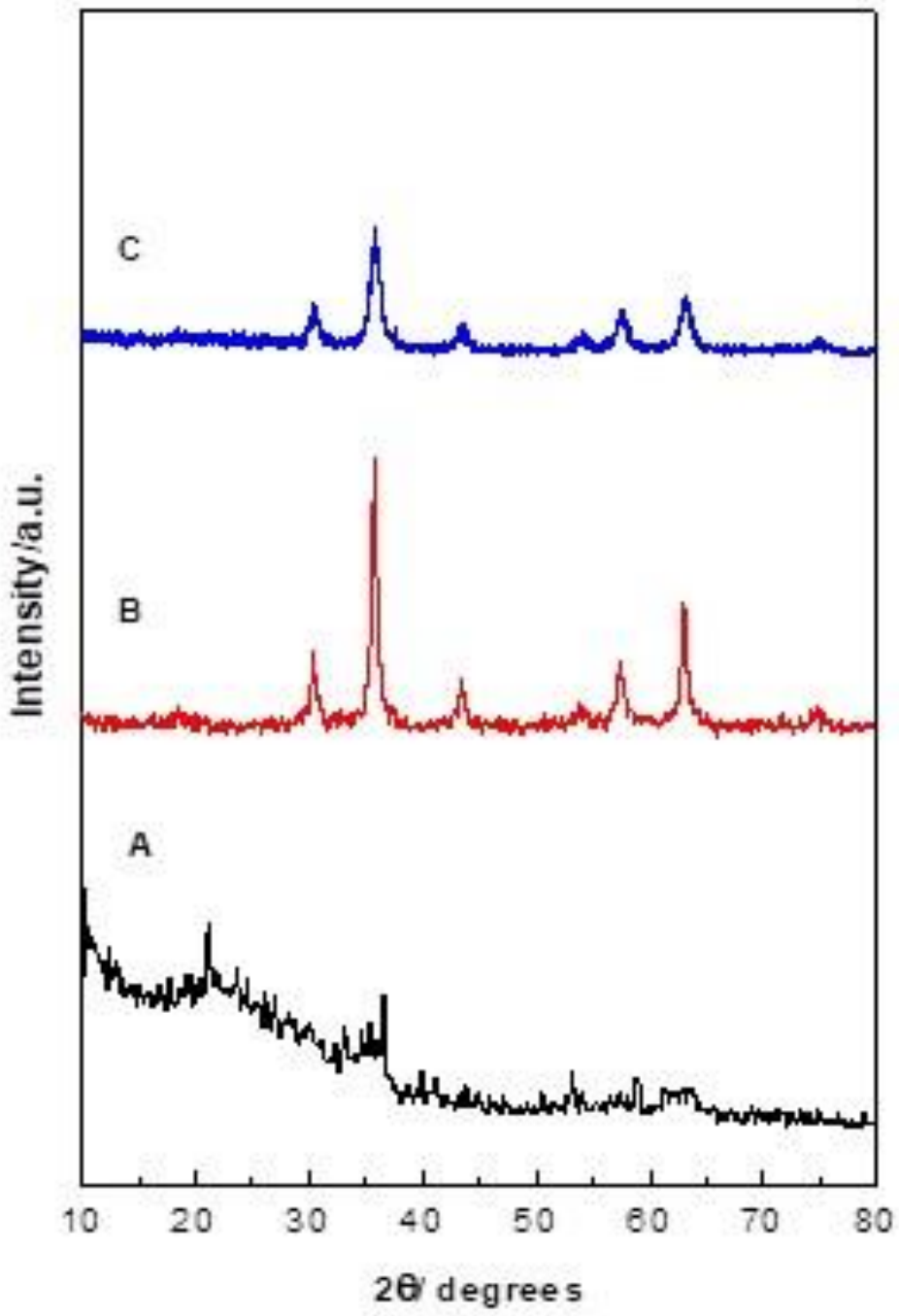

729 **Graphical Abstract**

730

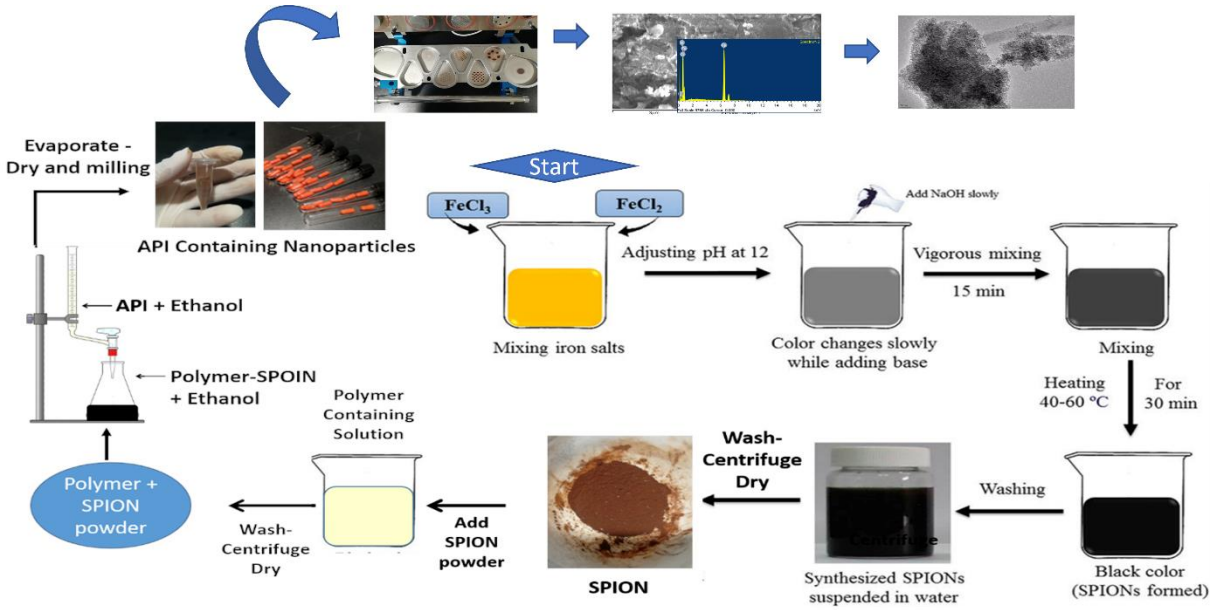

731

732